

The Geometry and Dynamics of Binary Trees

T. David¹, Thomas van Kempen¹, HuaXiong Huang², Phil Wilson³,

¹Centre for Bioengineering, University of Canterbury, New Zealand, ²Department of Mathematics and Statistics, York University, Toronto Canada, ³Department of Mathematics and Statistics, University of Canterbury, New Zealand.

Email: tim.david@canterbury.ac.nz

Abstract: The modeling of a fully populated 3D tree able to regulate dynamically remains a relatively unexplored field. A non-dimensional representation of “autoregulation” coupled with an asymmetric binary tree algorithm has been developed. The tree has a defined topology as well as a spatial representation in 3D. An analysis using a simple linearization shows the systems dynamics when perturbed away from equilibrium. Results, based on previously published work by Karch and Schreiner are presented for a variety of parameters which provide different shapes of the tree and indicate a possible mechanism for “growing” the tree in specified directions. In addition the tree, through the use of local tagging has the ability to vary it’s size locally via a coupled set of conservation and reverting differential equations.

Keywords: Binary tree, autoregulation, dynamics

1 INTRODUCTION

Binary trees (in which a node has two children) appear in nature quite naturally. Tree roots, the vascular beds of mammals (particularly the human brain, [1]) are physical examples. By virtue of their “living” condition the trees we consider, in a significant number of cases have the ability to change their size (effectively the radius of each segment of the tree). However the trees which we develop and analyse are defined from a computational science point of view as full rooted binary trees (<http://www.itl.nist.gov/div897/sqg/dads/HTML/completeBinaryTree.html>): but we do not consider here the binary trees associated with purely computational science reasons as will be shown below.

The present model in determining the developed binary tree uses previous work by Olufsen [2] Karch [3] and Schreiner [4]. In order to allow all parts of the tree to vary in its radius (and hence as will be shown resistance) the model is non-dimensionalised enabling a single algorithm to be utilized throughout the structure of the tree.

From a biological viewpoint mammalian tissue requires a constancy of both oxygen and nutrients. During periods of pressure variation, which occur throughout the normal day as well as in cases of pathological hypo- and hyper-tension, the body’s cerebral (for example) autoregulation mechanism cause the arterioles to vasoconstrict/dilate in response to changes in cerebral perfusion pressure over a certain range, thus maintaining a relatively constant cerebral blood flow. These effects are of particular importance when investigating how blood is redistributed not only via the circle of Willis but throughout the cerebral tissue.

In this paper we do **not** concentrate on the biological but investigate the dynamics of the binary tree from a general sense.

Although the work presented here is based upon the staged growth algorithms of Karch [3] the main differences are that the computational effort in producing a viable generic binary tree is much less than that of Karch (due to their complex optimization algorithm). Indeed the binary trees presented here may be easily parallelizable: so much so that a massively parallel architecture such as a Blue Gene can be utilised to its full potential (this will be the subject of a further paper).

2 THEORY AND METHODOLOGY

2.1 Asymmetric binary tree model

Basic Topology

The tree branching algorithm used is that developed for the abdominal fractal vascular network of Olufsen et al [2] and is based on two variables: a power exponent k (describing the relationship between parent segment

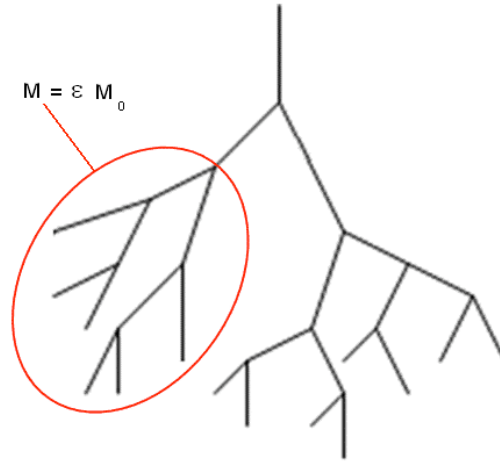


Figure 1: A local area of the tree with variation in the production rate

radius r_p and daughter segments radii r_{d1} and r_{d2} , defined by the following relation,

$$r_p^k = r_{d1}^k + r_{d2}^k \quad (1.1)$$

and an asymmetry ratio γ (describing the relative ratio between two daughter segments) defined as

$$\gamma = \left(\frac{r_{d2}}{r_{d1}} \right)^2 \quad (1.2)$$

With the foregoing equations, relations can be derived between the radii of the parent and daughters. These relations are,

$$\begin{aligned} r_{d1} &= \eta r_p \\ r_{d2} &= \nu r_p \end{aligned} \quad (1.3)$$

With

$$\eta = \left(1 + \gamma^{\frac{\kappa}{2}}\right)^{-\frac{1}{\kappa}} \quad (1.4)$$

$$\nu = \sqrt{\gamma\eta}$$

For this particular study a binary tree emulates the values of κ and γ change depending on the location of the segment in the tree. The length and radius of a segment are related by a length to radius ratio (denoted l_{rr} and chosen as 20 for this model). Here we take values of κ and γ as those given in [2]. Figure 1 shows a sketch of the basic network indicating an area of variable production rate. We call this particular tree an asymmetric tree as opposed to that where $\eta = \nu$.

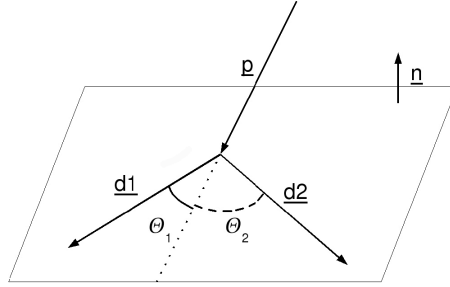


Figure 2: daughter segment angles and their corresponding plane

Additionally we are able to define trees in 3D by finding the coordinates of a daughter segment when it is born. With volume minimizing considerations, Kamiya and Togawa [5] showed in their studies that the angles $\theta_{1,2}$ (see Figure 2) between a parent and its daughters are a function of their radius as shown in equation (1.5).

$$\cos \theta_1 = \frac{r_p^4 + r_{d1}^4 - r_{d2}^4}{2r_p^2 r_{d1}^2} \quad (1.5)$$

$$\cos \theta_2 = \frac{r_p^4 + r_{d2}^4 - r_{d1}^4}{2r_p^2 r_{d2}^2}$$

For each daughter, there are three unknowns (the coordinates of the upper extremity) so three equations are needed. By fixing the length and this angle there are two equations. The last equation says that the two daughters belong to the same plane (n is the normal of this plane) and the coordinates of n are drawn randomly as described below in the section “Spatial Distribution of tree segments”. This randomization allows for “forcing” the arteries to grow in particular directions as used by Schreiner et al [4]. Hence we can write the following constraints

$$\begin{aligned} \langle d, n \rangle &= 0 \\ \|\mathbf{d}\|_2 &= L \\ \langle \mathbf{p}, \mathbf{d} \rangle &= \cos \theta \|\mathbf{d}\|_2 \|\mathbf{p}\|_2 \end{aligned} \quad (1.6)$$

with \mathbf{d} the vector representing the daughter and \mathbf{p} the projection of the parent on the plane of the daughters. Unfortunately, this system is non-linear and hence solved with an iterative method. The Newton-Raphson method has been chosen in this case.

Now $\mathbf{F}(\mathbf{d}) = 0$ is solved using a Newton-Raphson algorithm where $\mathbf{F} : \mathbb{R}^3 \rightarrow \mathbb{R}^3$ is defined by

$$\mathbf{F}(\mathbf{d}) = \begin{pmatrix} xn_x + yn_y + zn_z \\ x^2 + y^2 + z^2 - L^2 \\ xp_x + yp_y + zp_z - \cos\theta L\|\mathbf{p}\|_2 \end{pmatrix}; \mathbf{d} = \begin{pmatrix} x \\ y \\ z \end{pmatrix}, \mathbf{p} = \begin{pmatrix} p_x \\ p_y \\ p_z \end{pmatrix} \text{ and } \mathbf{n} = \begin{pmatrix} n_x \\ n_y \\ n_z \end{pmatrix} \quad (1.7)$$

Spatial Distribution of tree segments

As explained above, the daughters are forced to grow in a plane with normal \mathbf{n} . The components of this normal are drawn randomly from a uniform distribution. In this study the components of the normal are chosen such that the tree grows in a more controllable fashion. An algorithm, called staged growth and published by Karch *et al.* [3], is used to develop this concept. The main idea is that the components of the normal are drawn from a certain distribution (e.g. a normal distribution) such that the daughters are forced to grow in a certain direction and the geometry of the tree can be controlled. Karch *et al.* [3] use the concept of staged growth to create models of the coronary arterial tree. Some ideas of this concept are applied to the models described in this study. The main idea is that a random variable, in this case one or more components of the normal, are drawn according to a certain distribution. This distribution changes during the development of the tree i.e. there are different stages of growth. Below we explain how the z-component of the normal, n_z , is drawn according to this concept but it has to be mentioned that exactly the same can and will be done to the components n_x and n_y .

Let's assume one wants to draw n_z according to a certain distribution with probability density function (PDF) $g(n_z)$. Different stages of growth can be realized by making the PDF a function of a parameter λ , i.e. $g = g(n_z, \lambda)$ with $\lambda \in [0, 1]$. By changing the value of λ , the PDF of n_z is changed. The parameter λ determines the stage of growth the process is in, and gives for each stage of growth a PDF $g = g(n_z, \lambda)$. In order to let a function be a PDF, the function has to be non-negative over the whole interval and the integral over the whole interval has to equal one. Since the function $g(n_z, \lambda)$ is defined as a PDF, it satisfies these conditions,

$$\begin{aligned} g(n_z, \lambda) &\geq 0 \\ \text{and} & \\ \int_{\mathbb{R}} g(n_z, \lambda) dn_z &= 1 \end{aligned} \quad (1.8)$$

If it is assumed that λ is given according to a PDF $p(\lambda)$ then

$$p(\lambda) \geq 0, \quad \int_0^1 p(\lambda) d\lambda = 1 \quad (1.9)$$

The overall PDF is written as

$$f(n_z) = \int_0^1 p(\lambda) g(n_z, \lambda) d\lambda \geq 0 \quad (1.10)$$

With equations (2.13) and (2.15) it follows that

$$\int_{\mathbb{R}} f(n_z) dn_z = \int_{\mathbb{R}} \int_0^1 p(\lambda) g(n_z, \lambda) d\lambda = 1 \quad (1.11)$$

hence $f(n_z)$ is properly normalized and satisfies the conditions of a PDF. Equation (1.9) suggests that the value of λ , is chosen randomly from a distribution with PDF $p(\lambda)$. This is in general not the case, since the value for λ , is generated by a protocol function $\lambda(t)$.

$$\lambda : [0,1] \rightarrow [0,1], \quad t \rightarrow \lambda(t) \quad (1.12)$$

Constraints to this function $\lambda(t)$ are that it has to be bounded and at least piece-wise continuous. The parameter t can be seen as a normalized 'time', a value that changes from zero to one during the development of the tree. The value of t has to be related to a quantity that changes during the development of the tree. The only quantity of the final tree that is known in the beginning of the growing process is the radius of the terminal segments, r_N , since this is used as the stop criterion for the algorithm. Therefore it is chosen to relate the variable t to the radius r of a certain segment and a function is needed that maps the radius of a segment to a value t ,

$$\begin{aligned} t : [r_N, r_1] &\rightarrow [0,1], \quad r \rightarrow t(r) \\ t(r) &= \frac{r_1 - r}{r_1 - r_N} \end{aligned} \quad (1.13)$$

The concept of staged growth can be summarized as follows. For a segment with radius r , the value for t is given by the function $t(r)$, equation (1.13). The next step is to define the functions $\lambda(t)$ and $g(n_z, \lambda)$.

An example of a protocol and probability density function

The functions $g(n_z, \lambda)$ and $\lambda(t)$ are initially chosen the same as that suggested by Karch et al. [20]. They suggest functions that create an overall uniform distribution of the variable, i.e. $f(n_z) = 1$. In this study it is not necessary to aim for a uniform overall distribution of n_z but the same functions for $g(n_z, \lambda)$ and $\lambda(t)$ are used nevertheless as a starting point and the reader is referred to the work of Karch et al. [3] for the motivation behind the choice of these functions.

To start with, the function $g(n_z, \lambda)$ is defined as a powerlaw function,

$$g(n_z, \lambda) = \frac{2n_z}{\lambda^2} H(\lambda - n_z) \quad (1.14)$$

In which $H(\lambda - n_z)$ represents the Heaviside function. For the "protocol" function $\lambda(t)$ a ramp function is used such that

$$\lambda(t) = \begin{cases} 2t & \text{for } 0 < t \leq \frac{1}{2} \\ 1 & \text{for } \frac{1}{2} < t \leq 1 \end{cases} \quad (1.15)$$

With equations (1.13), (1.14) and (1.15) a PDF $g(n_z, \lambda)$ is defined for each segment of the tree. The next step is to sample n_z such that it satisfies the probability density $g(n_z, \lambda)$. This is accomplished by choosing a random number $\xi \in [0, 1)$ and an inverse transformation $n_z = n_z(\xi)$ [20]. This transformation is found by using the cumulative distribution functions (CPDF) of n_z and ξ . Since ξ is uniformly distributed, its CPDF $F(\xi)$ is given by,

$$F(\xi) = \xi \quad (1.16)$$

The CPDF $g(n_z, \lambda)$ is given by,

$$\begin{aligned} G(n_z, \lambda) &= \int_0^{n_z} g(u, \lambda) du \\ &= \int_0^{n_z} \frac{2u}{\lambda^2} du = \frac{n_z^2}{\lambda^2} \end{aligned} \quad (1.17)$$

The transformation $n_z = n_z(\xi)$ is found by equating $F(\xi)$ to $G(n_z, \lambda)$,

$$n_z = \lambda \sqrt{\xi} \quad (1.18)$$

As a consequence of the transformation $n_z(\xi)$, the value for n_z is always positive i.e $n_z \in [0, 1)$. This raises the question of the influence of the sign and magnitude of a component n_i on the direction of growth of the daughters. To answer this question different options are proposed to scale the value of n_z . Two options are given that scale n_z to $n_z \in (-1, 1)$ and a third option is to use no scaling, $n_z \in [0, 1)$. The three investigated options are,

Option 1:

$$n_z = s\lambda\sqrt{\xi}, \quad n_z \in (-1, 1) \quad (1.19)$$

in which $s \in (-1, 1)$. The value of s is chosen as follows. A random variable $\zeta \in [0, 1)$ is sampled from a uniform distribution. If $\zeta < 0.5$, $s = -1$ else $s = 1$

Option 2:

$$n_z = -1 + 2\lambda\sqrt{\xi}, \quad n_z \in (-1,1) \quad (1.20)$$

Option 3

$$n_z = \lambda\sqrt{\xi} \quad n_z \in [0,1) \quad (1.21)$$

It has to be mentioned that these three options are chosen because they are expected to be illustrative for the influence of different values of n_z , not because they are the only possible options. There are many other ways to define the relation between n_z and λ , but these are not taken into account in this study. It is expected that the magnitude of n_z has more influence than its sign on the final outcome of the tree. This hypothesis can be easily tested by comparing trees generated with the three options described before. The hypothesis stated above can only be used when one of the components of the normal is varied. When more than one component is varied, the direction of the normal changes in multiple directions and the stated situation above is not valid.

With the foregoing steps, the components of the normal n can be drawn according to a distribution with PDF $g(n_z, \lambda)$. The protocol function $\lambda(t)$ determines the different stages of growth. Thus far, only a powerlaw PDF and a ramp protocol function are discussed but there are more possibilities for these functions. These are described in the next section.

Other protocol and probability density functions

The powerlaw PDF (equation (1.14)) and the ramp protocol function (equation (1.15)) are chosen as illustrative examples to get familiar with the concept of staged growth but there are many more possibilities for these functions. Since these functions are expected to influence the final shape of the tree, different functions are proposed to investigate this influence. To get more sense about the influence of the parameter λ , the protocol function $\lambda(t)$ is defined as a simple Heaviside step function,

$$\lambda(t) = \begin{cases} 0 & \text{for } 0 < t \leq \frac{1}{2} \\ 1 & \text{for } \frac{1}{2} < t \leq 1 \end{cases} \quad (1.22)$$

Since the transition between the two stages is more emphasized in this protocol function than in equation (1.15), it is expected that trees generated with this protocol function show a clearer transition between the two stages. By choosing the function $g(n_z, \lambda)$ to be a powerlaw function, the value of n_z has a value between zero and λ . It would therefore be more reasonable to give n_z a mean value related to λ , with a certain deviation from this value. This can be realized by defining $g(n_z, \lambda)$ as the PDF of a normal distribution. By choosing the mean of the distribution equal to λ , the value of n_z will be equal to λ , plus or minus a variation (whose value can be chosen a priori). The PDF of a normal distribution is given by,

$$g(n_z, \lambda) = \frac{1}{\sigma\sqrt{2\pi}} \exp\left\{-\frac{n_z - \lambda^2}{2\sigma^2}\right\} \quad (1.23)$$

in which σ is the standard deviation of the distribution. The normal PDF is shown for different values of λ , and $\sigma = 0.1$. The next step is to sample n_z such that it satisfies the normal PDF. This is done using the same kind of transformation as used with the powerlaw PDF i.e. a transformation $n_z(\xi)$ in which ξ is a randomly chosen value from a uniform distribution. The CPDF of ξ is given by equation (1.16). The CPDF of $g(n_z, \lambda)$ is given by ,

$$\begin{aligned} G(n_z, \lambda) &= \int_{-\infty}^{n_z} \frac{1}{\sigma\sqrt{2\pi}} \exp\left\{-\frac{u-\lambda^2}{2\sigma^2}\right\} du \\ &= \frac{1}{2} \left(1 + \operatorname{erf}\left(\frac{n_z - \lambda}{\sqrt{2}\sigma}\right)\right) \end{aligned} \quad (1.24)$$

in which $\operatorname{erf}(x)$ is the error function. This results in,

$$n_z = \lambda + \sqrt{2}\sigma \operatorname{erf}^{-1}(2\xi - 1) \quad (1.25)$$

The inverse error function, $\operatorname{erf}^{-1}(x)$ is not defined for $x = \pm 1$. This gives constraints to the randomly chosen variable ξ , since in equation (1.25), the value of $(2\xi - 1)$ has to be between -1 and +1. This subtle difference with the situation of the powerlaw PDF has to be taken into account during the implementation. There are again three different options to scale the value of n_z . These options are analogous to the three options used with the powerlaw PDF above. The parameter ε denotes the deviation from the mean value.

Option 1:

$$n_z = s\lambda + \sqrt{2}\sigma \operatorname{erf}^{-1}(2\xi - 1), \quad n_z \in (-1 - \varepsilon, 1 + \varepsilon) \quad (1.26)$$

in which $s \in (-1, 1)$, identical to option 1 of the powerlaw PDF.

Option 2:

$$n_z = -1 + 2\lambda + \sqrt{2}\sigma \operatorname{erf}^{-1}(2\xi - 1), \quad n_z \in (-1 - \varepsilon, 1 + \varepsilon) \quad (1.27)$$

Option 3:

$$n_z = \lambda + \sqrt{2}\sigma \operatorname{erf}^{-1}(2\xi - 1), \quad n_z \in (-1 - \varepsilon, 1 + \varepsilon) \quad (1.28)$$

The inverse error function is a function that cannot be defined explicitly, however many numerical approximations are available. In this study the approximation proposed by Winitzki [6] is used which gives a maximum relative error of 4×10^{-3} . With the concept of staged growth, it is possible to change one or more components of the normal \mathbf{n} . This concept will be used to gain more control of the direction of growth of the different daughter segments of the tree. In the results section, different trees will be presented, generated with the PDFs and protocol functions as described above. One or more components of the normal will be chosen according to the concept of stage growth in order to get an insight in the exact behavior of the trees under different conditions.

One final remark should be made. When one or more components of the normal are determined by using the concept of staged growth, the other component(s) are chosen randomly from a uniform distribution and given a value between -1 and +1.

The process described in the foregoing sections is implemented in C++, using the Lapack++ [7] library for vector and matrix manipulations. A class segment is created which contains the following attributes:

- A pointer to the segments parent.
- Two pointers to the segments daughters.
- The segments radius.
- The coordinates of the segments end-point.
- The segments level i.e. the number of antecedents it has.
- A tag that will be used to distinguish segments from others.

Figures 3a) and 3b) show examples of trees grown in 3D with varying sizes of root segment (the terminating segment size was always $10 \mu m$)

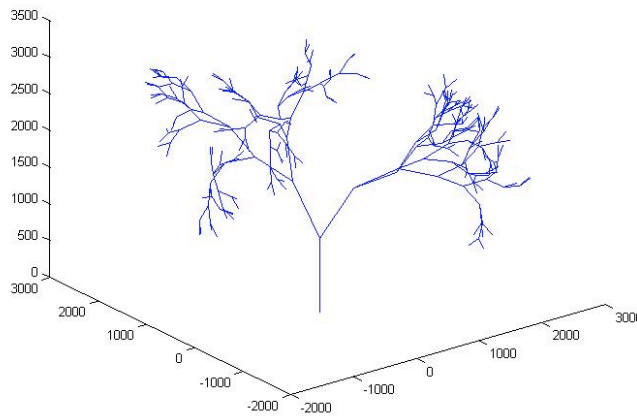


Figure 3a) 313 segments

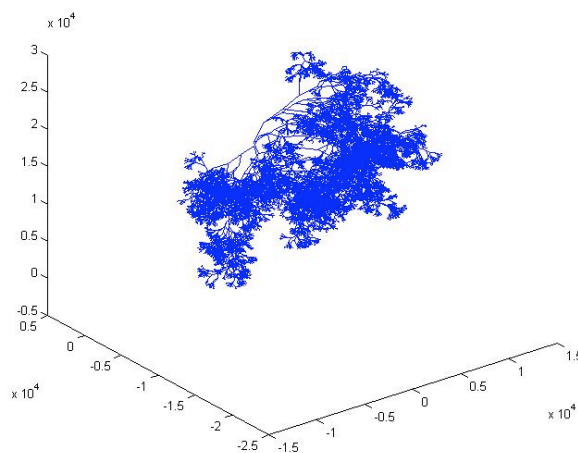


Figure 3b) 13,987 segments

2.2 Conservation “flow” Model

In order for the tree to change its radii under changes to an equilibrium state we require a differential equation (or more than one) to model the dynamic state of the tree segments and that of the tree as a whole. For the sake of simplicity we introduce a fictional “concentration” which can be thought of in a number of physical manifestations such as water flow in a plant root or blood flow in an arterial bed [8]. We therefore introduce a conservation differential equation (defined over a small domain, for this case a segment of the tree) for this fictional concentration by allowing the concentration to be produced at some rate M , which we will call the “production” rate. To balance this rate of production we also introduce a means of allowing the concentration to “flow” away from the elemental domain in proportion to its excess above some nominal value using the constant of proportionality as a “flow”, F . Hence the conservation of the concentration C can be defined thus,

$$\frac{dC}{dt} = M + F(C_{norm} - C) \quad (1.29)$$

In order to couple the variation of concentration with a change in radius of the segments of the tree we use a reverting differential equation for the radius of the segment given by

$$\frac{dr}{dt} = \frac{1}{\tau}(C_{eq} - C) \quad (1.30)$$

here C_{eq} is the steady state ($\frac{dC}{dt} = 0$) solution to (1.29) where τ is a characteristic time for the segment radius to react. We choose the following non-dimensionalisation

$$c = \frac{C}{C_{norm}}; t = \frac{T}{F_0}; \xi = \frac{r}{r_0} \quad (1.31)$$

where r_0 is the leaf radius and F_0 is the value of the “flow” in the terminating segment (leaf) at some prescribed conditions. With the above equations (1.29) and (1.30) become

$$\begin{aligned} \frac{dc}{dT} &= (\psi - 1) + Q(1 - c); \\ \frac{d\xi}{dT} &= -\xi(\psi - c) \end{aligned} \quad (1.32)$$

With

$$Q = \frac{F}{F_0}; \psi = 1 + \frac{M}{C_{norm}F_0}; \xi = \frac{C_{norm}}{\tau r_0 F_0} \quad (1.33)$$

We generate a more appropriate time-scale to make the equations easier to handle such that

$$\tau = T\xi \quad (1.34)$$

Then we have

$$\begin{aligned}\frac{dc_i}{d\tau} &= \alpha + \beta Q_i (1 - c_i) \\ \frac{dr_i}{d\tau} &= c_i - c_{i,eq}\end{aligned}\tag{1.35}$$

Here the i 'th subscript indicates the radius and ‘‘concentration’’ at the i 'th branch level of the tree. We introduce two additional terms into the radius equation. The first term allows only a certain bounded radius whilst the second term ensures that there radius returns to its equilibrium value. So finally we have

$$\begin{aligned}\frac{dc_i}{d\tau} &= \alpha + \beta (1 - c_i) \\ \frac{dr_i}{d\tau} &= \left(c_i - 1 - \frac{\alpha}{\beta} \right) \left([H(r_i - r_{\min})] [H(r_{\max} - r_i)] \right) + \gamma_i (r_{i,eq} - r_i) \exp \left\{ \frac{\left(c_i - 1 - \frac{\alpha}{\beta} \right)^2}{\epsilon} \right\}\end{aligned}\tag{1.36}$$

2.3 ‘‘Tagging’’ the tree

We may wish to investigate the dynamics of the tree when the values of M are varied in the tree, rather than it being a global constant. The tree segments that have a changed value of M get a tag to distinguish them from others and are therefore called ‘tagged’ segments. There are two methods introduced to decide if a segment is a tagged segment or not. The first method is based on the location of the endpoint of a segment in the 3D space. A point is chosen in the 3D space and all segments whose end point is located within a sphere around this point get a tag. The radius of the sphere can be varied to change the amount of tagged segments. Because the tagging is only based on the location of a segment it is possible that not all segments downstream of a tagged segment get a tag which might be incorrect from a physiological point of view.

A problem with this method is that it is unknown in which direction the tree will grow on beforehand, due to the random element in the algorithm that generates the tree. This makes it impossible to choose a reasonable center for the sphere before the tree is generated. This problem is solved by removing the random element in the code (by not initializing the random number generator), resulting in the same tree every time the code is executed. When the tree is generated, it is visualized and a point in the 3D space is chosen that will function as the center of the sphere during the next execution of the code. With this method, segments can be tagged in a controlled region of the tree. This method is called region-tagging. The second method used to tag segments is based on the antecedents a segment has. A single segment in a certain level is tagged, together with all of its offspring. This method will be called antecedent-tagging. The difference between the two methods is that with region-tagging, the segments are located all in the same spatial region but are not necessarily antecedents of the same segment. In the second case, the segments are antecedents of one single segment, but they are not necessarily located in the same spatial region.

2.4 Resistance and pressure distributions in the tree

To find each individual resistance to flow of each segment in the tree it is convenient to use a Poiseuille flow assumption such that the resistance of a tree segment is proportional to the inverse of the fourth power of the radius. In order to find the flow and pressure distribution throughout the tree a single pass up and down the tree is required. Starting at each terminal segment a total resistance is evaluated for the two daughters and the parent segment assuming that the terminal segments are connected (essentially daughters in parallel with the parent in series) together where a constant pressure is set. This parallel/series calculation is then done at each bifurcation of the tree until there is a single value of resistance. The total flow into the arterial tree is known and hence the total pressure drop can be evaluated or vice versa. Moving down the tree the pressure drop and

flow rate at and through each arterial segment is calculated respectively. The trees used to produce the results in this paper vary in size however we have been able to create trees that consist of approximately 1,000,000 segments of which 500,000 are terminal segments.

2.5 Dynamical Analysis

It is necessary to analyse the dynamics of the tree and to use these results to compare with the full non-linear numerical solutions shown below in section 4. For this analysis we assume that the tree is symmetrical (daughters have the same radii). Suppose that daughters branch with a parent/daughter radius ratio of ϕ s.t.

$$\begin{aligned} r_{2,eq} &= \phi^{-1} r_{1,eq} \\ r_{j,eq} &= \phi^{N-j} r_{1,eq} = \phi^{N-j} \end{aligned} \quad (1.37)$$

since we have non-dimensionalised by the leaf radius. Turning to the “flow” in the tree we have in a similar fashion to the radius that

$$Q_i = 2^{1-i} Q_1 = 2^{1-i} \left(\sum_{j=1}^N \frac{R_j}{2^{j-1}} \right) \quad (1.38)$$

Where R_j is a resistance to “flow” such that $R_j \propto \frac{1}{r_j^3}$ and N is the total number of branches in the tree.

It is easy to show that the equilibrium “flow” can be written as

$$Q_{i,eq} = 2^{1-i} Q_{1,eq} = 2^{1-i} \left(\sum_{j=1}^N (\phi^{j-N})^3 2^{1-j} \right)^{-1} = 2^{N-i} \frac{2\phi^3 - 1}{(2\phi^3)^N - 1} \quad (1.39)$$

We can now turn to analysing the eigenvalues of the system which helps determine the dynamics of the tree when perturbed away from an equilibrium state. Firstly we determine the Jacobian of the system by defining the two equations thus,

$$\begin{aligned} g_1 &:= \frac{dr_i}{d\tau} = \left(c_i - 1 - \frac{\alpha}{\beta} \right) + \gamma_i (r_{i,eq} - r_i) \exp \left\{ \frac{\left(c_i - 1 - \frac{\alpha}{\beta} \right)^2}{\varepsilon} \right\} \\ g_2 &:= \frac{dc_i}{d\tau} = \alpha + \beta (1 - c_i) \end{aligned} \quad (1.40)$$

$$\left. \frac{dg_1}{dc_i} \right|_{eq} = 1; \quad \left. \frac{dg_1}{dr_i} \right|_{eq} = \gamma_i \exp \left\{ \frac{\left(c_i - 1 - \frac{\alpha}{\beta} \right)^2}{\varepsilon} \right\} \quad (1.41)$$

$$\left. \frac{dg_2}{dc_i} \right|_{eq} = -\beta; \quad \left. \frac{dg_2}{dr_i} \right|_{eq} = \frac{-\alpha}{Q_{i,eq}} \left. \frac{\partial Q_i}{\partial r_i} \right|_{eq} = -3\alpha \frac{2\phi^3 - 1}{(2\phi^3)^N - 1} (2\phi^4)^{N-i} = -\delta_i$$

$$\mathbf{J} - \lambda \mathbf{I} = \begin{bmatrix} -(\gamma_1 + \lambda) & 1 & & & 0 \\ 0 & \ddots & \ddots & & \vdots \\ \vdots & & -(\gamma_N + \lambda) & 1 & \vdots \\ \vdots & & & -(\beta + \lambda) - \frac{\delta_1}{(\gamma_1 + \lambda)} & \vdots \\ \vdots & & & & \ddots & \vdots \\ 0 & \dots & \dots & \dots & 0 & -(\beta + \lambda) - \frac{\delta_N}{(\gamma_N + \lambda)} \end{bmatrix} \quad (1.42)$$

By allowing the determinant of the matrix to be zero and thereby avoiding trivial solutions we find that the eigenvalues of the system are given by

$$\begin{aligned} \lambda_i &= \frac{1}{2} [-(\gamma_i + \beta) \pm i\omega_i] \\ \omega_i &= 4\delta_i - (\gamma_i + \beta)^2 \end{aligned} \quad (1.43)$$

Hence the perturbation solution has the form

$$y = e^{\lambda t} = \exp \{ -(\gamma_i + \beta)t \} \cos(\sqrt{\omega_i}t) \quad (1.44)$$

Figure 4a) shows the profile of the radius of the tree leaf with $\gamma_i = 0$. There exists a small undershoot (maximum at approx $t = 5$) before the radius is returned to its equilibrium value at $t = 10$.

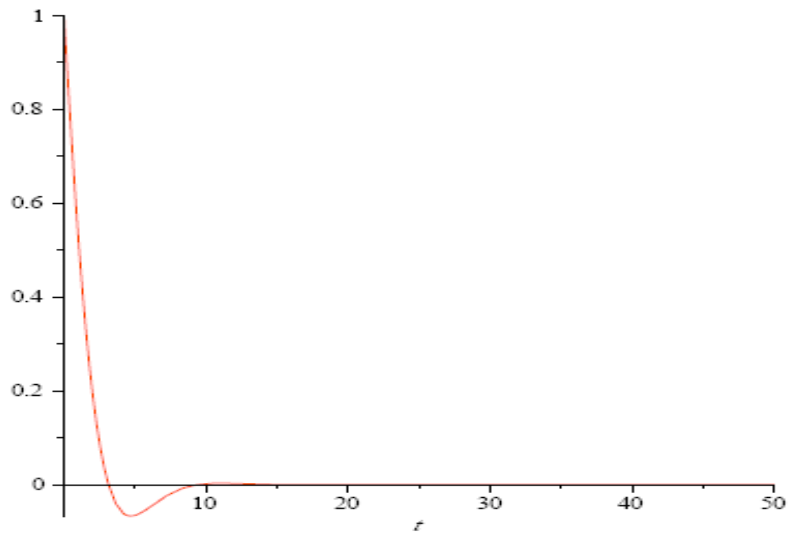


Figure 4a perturbation solution for leaf ($i=N$) with $\gamma_i = 0$

Figure 4b shows the radial profile for a leaf of the tree when $\gamma_i = 0.2$. Here the undershoot previously seen is greatly reduced as the exponential index has increased negatively due to the presence of the non-zero value of γ_i .

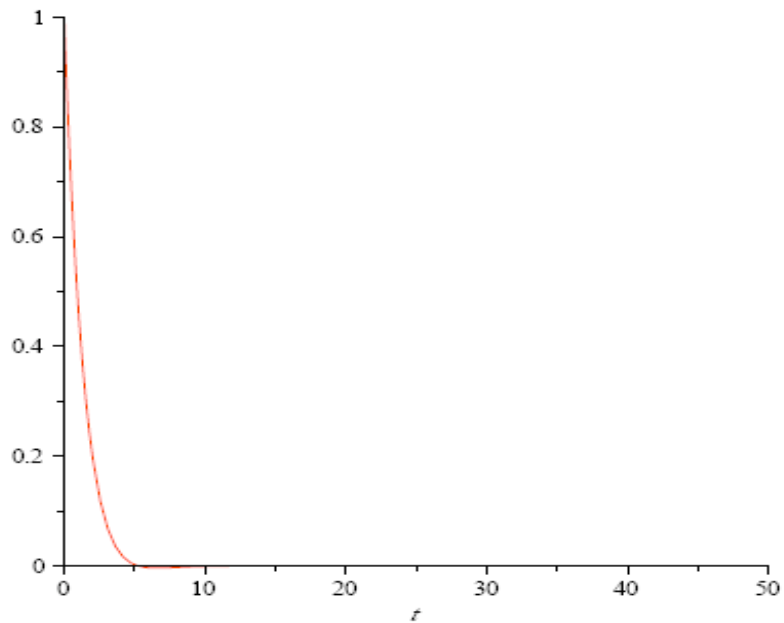


Figure 4b perturbation solution for leaf ($i=N$) with $\gamma_i = 0.2$

3 NUMERICAL METHODS

The differential equations (1.29) and (1.30), were solved using MATLAB's ode23s routine (based on a modified Rosenbrock formula of order 2).

3.1 Solution of autoregulation model with the asymmetric binary tree

All initial flow rates, pressure drops, and radii of all tree segments are calculated at the creation of the arterial tree as described above and using a known value of the initial radius (in this case determined by the branching level and the choice of a leaf radius which was constant at $10\mu m$) and a unit pressure. All

pressures and flow are then recalculated throughout the arterial tree with these new radii values by traversing up and down the tree to evaluate new pressures and flow rates. This process is then repeated until a simple convergence criterion on the total peripheral resistance is met.

4 RESULTS

Visualisation of the binary Trees

There are three different methods used to visualize and describe a vascular tree generated with the concept of staged growth. The first is a graphical view of the tree in which the viewpoint is positioned in any desirable direction. In order to get a more quantitative description of the tree, the distribution of the z-coordinate of the terminal segments is used (in some cases, the distribution of the y-coordinate of the terminal segments is used). The third way of representing a tree is the distribution of the angles that the daughters make with their parent. All trees have a root segment with radius $r_{root} = 100\mu m$ and a terminal radius of $r_{term} = 10\mu m$. The root segment starts at the origin and points in the positive z-direction. Trees with a root- and terminal radius as stated above, consist of 2061 segments, divided in 13 levels i.e. a terminal segment has maximal 13 antecedents. Unless stated otherwise, the only component of the normal n that is varied is n_z . Because of the random element in the algorithm, two trees generated with the same settings are never the same. Results are shown of trees that are representative for certain settings but it has to be kept in mind that there is always variation between different trees generated with the same settings.

4.1 Angles between daughter and parent

It can be shown that Option 2 produces trees that grow in negative z-direction and is in the sense of this analysis a redundant case. Therefore, it is chosen to not analyze option 2 further and to focus on options 1 and 3. To investigate the difference between option 1 and 3 in more detail, ten trees are generated for each option. For each tree, the mean and standard deviations for the angles between daughter and parent are determined. For the angle distribution the kurtosis is computed as well. These values are averaged over the ten trees generated with the same option. The results of this analysis is shown in Table 1

Table 1

θ (degrees)	Option 1	Option 3
Mean	56.47 ± 0.57	56.47 ± 0.52
Standard Deviation	18.19 ± 0.28	18.19 ± 0.31
Kurtosis	18.95 ± 3.05	16.92 ± 4.65

The results in table 1 show that there is little difference between the angle distributions of option 1 and 3. The mean and standard deviation of the distributions are surprisingly close to each other while the kurtosis is lower for option 3.

4.2 Powerlaw PDF and normal PDF

In figure 5, a graphical view can be seen of trees generated with a powerlaw PDF (left) and a normal PDF (right) both generated with the use of option 1, i.e the transformation between ξ and n_z is such that $n_z \in (-1, 1)$ for the powerlaw PDF and $n_z \in (-1 - \varepsilon, 1 + \varepsilon)$ for the normal PDF.

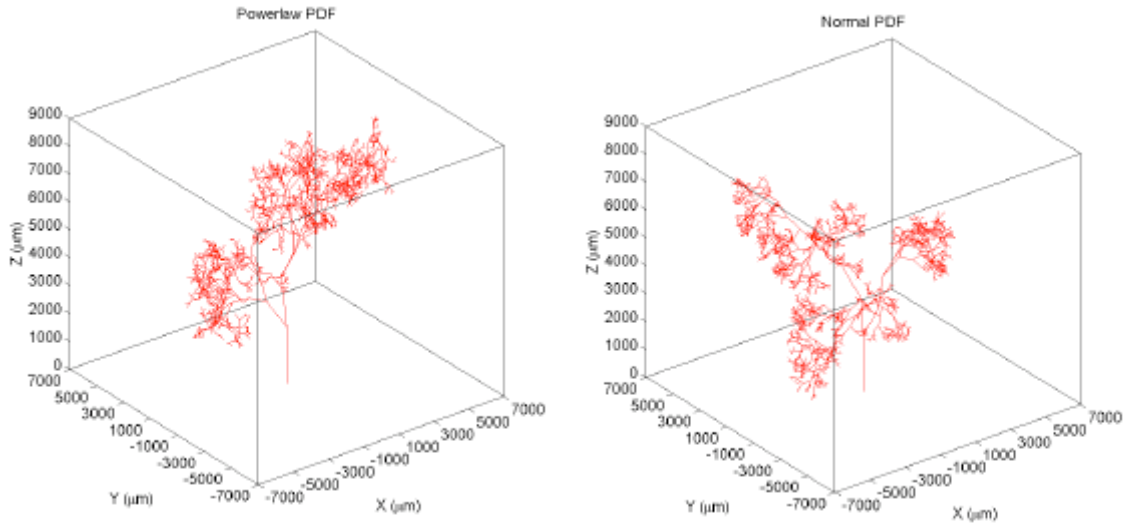


Figure 5 Trees generated with a powerlaw PDF (left) and the normal PDF (right).

Two different protocol functions (ramp function, and step function) are compared. For each protocol function, a tree is shown generated with a normal PDF and using option 1 for the scaling. In figure 6 the graphical views of the two trees can be seen.

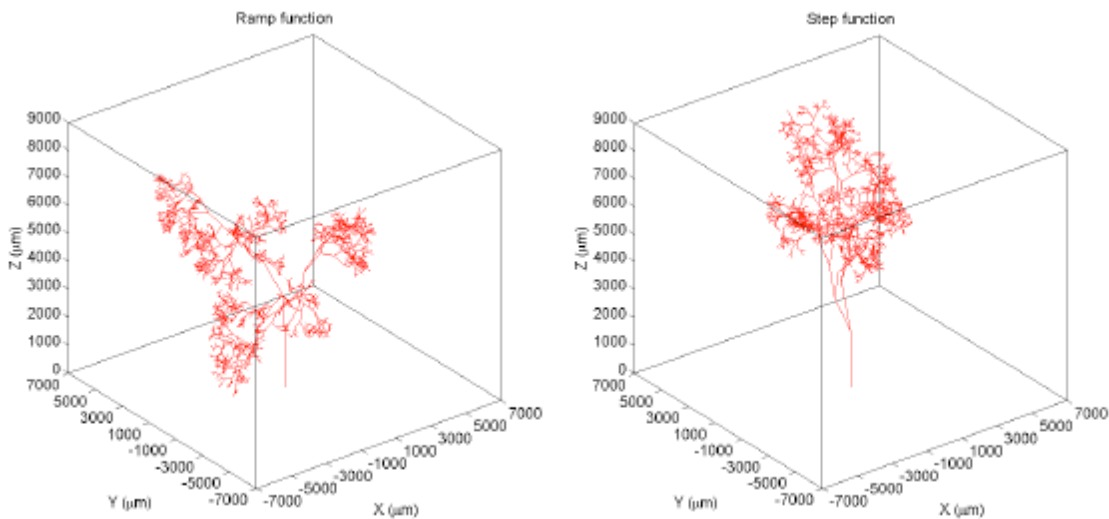


Figure 6 Trees generated with the ramp protocol function (left) and the step protocol function (right).

4.3 Varying multiple components of the normal

As a last variation, in this section multiple components of the normal \mathbf{n} are varied. The first variation is a tree in which the n_y, n_z components are chosen according to the concept of staged growth (with a normal PDF, option 1 and a step function as the protocol function). The n_x component is drawn randomly from a uniform distribution (as usual). During the first stage of growth, the segments grow in a plane with normal $\mathbf{n} = (n_x, \varepsilon, \varepsilon)$ in which ε is the deviation caused by the normal PDF. During the second stage of growth,

the segments grow in a plane with normal $\mathbf{n} = (n_x, 1 + \varepsilon, 1 + \varepsilon)$. This is summarized in the following equation,

$$\mathbf{n} = \begin{cases} (n_x, \varepsilon, \varepsilon) & \text{for } 0 < t \leq \frac{1}{2} \\ (n_x, 1 + \varepsilon, 1 + \varepsilon) & \text{for } \frac{1}{2} < t \leq 1 \end{cases} \quad (3.1)$$

in which t is defined by equation (1.13) and ε is the deviation caused by the normal PDF. The component n_x is drawn from a uniform distribution. A graphical view of this tree in negative z -direction can be seen in Figure 7, left.

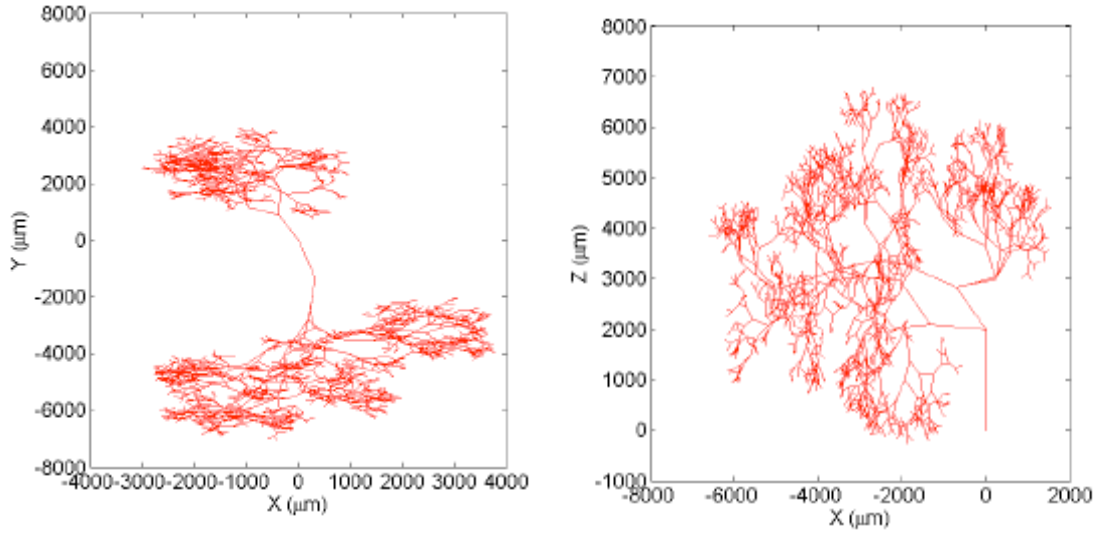


Figure 7 Two trees generated while multiple components of the normal are varied according to the concept of staged growth. In the left tree, the n_y and n_z component are varied, while in the right tree the n_x and n_y component are varied.

Another variation is a tree in which the n_x and n_y components of the normal are chosen according to the concept of staged growth (same settings as the previously mentioned tree) and the n_z component according to a uniform distribution. The difference with the previously mentioned tree is the orientation of the planes in which the tree grows, relative to the root segment. During the first stage of growth, the normals are given by $\mathbf{n} = (\varepsilon, \varepsilon, n_z)$, forcing the segments to grow in a plane close to the (x,y) -plane. During the second stage of growth, the segments grow in a plane with normal $\mathbf{n} = (1 + \varepsilon, 1 + \varepsilon, n_z)$. This is summarized in the following equation

$$\mathbf{n} = \begin{cases} (\varepsilon, \varepsilon, n_z) & \text{for } 0 < t \leq \frac{1}{2} \\ (1 + \varepsilon, 1 + \varepsilon, n_z) & \text{for } \frac{1}{2} < t \leq 1 \end{cases} \quad (3.2)$$

The result can be seen in Figure 7, right, in which the point-of-view is positioned such that the viewer looks in positive y -direction. Figure 7, left, shows that the tree generated with the n_y and n_z components chosen according to the concept of staged growth, grows in positive and negative y -direction during the first stage of growth. During the second stage, the tree spreads out in x -direction. In the right panel of the same figure, a view in positive y -direction can be seen of a tree generated with the n_x and n_y components chosen according to the concept of staged growth. The segments created during the first stage, grow mainly in a direction parallel to the x -axis. During the second stage, the segments spread out and grow in planes close to the (y,z) -plane. So far, the different PDFs (powerlaw and normal) and the three different options to scale n_z have been investigated. As a last step, different components of the normal \mathbf{n} have been varied. All variations have influence on the final geometry of the tree albeit some more than others. For instance, the difference between the tree generated with option 1 and 3 is very small while a change of protocol function has a big influence.

4.4 Variations in “Production” rate

In this section the results are shown for the simulations in which the “production” rate is changed by a factor ε for some of the segments between $t = t_0$ and $t = t_1$. As described there are two methods available to distinguish segments with a changed production rate (the tagged segments) from the segments that have a constant production rate (the non-tagged segments). The first method is to tag all segments within a sphere around a defined point. This method is called region tagging. The second method is called antecedent tagging and with this method all segments that are offspring of a certain segment are tagged.

To get more insight in the individual behavior of the vessels, Figure 8, shows a plot of the tree during the simulation with a local increase of the “production” rate of 50%. The colors indicate the radius of the vessels normalized to their initial value. The situation is shown at $t = 15$, the moment where the tree has reached a steady state after the production rate is increased by 50%. The vessels are tagged with the method of antecedent tagging.

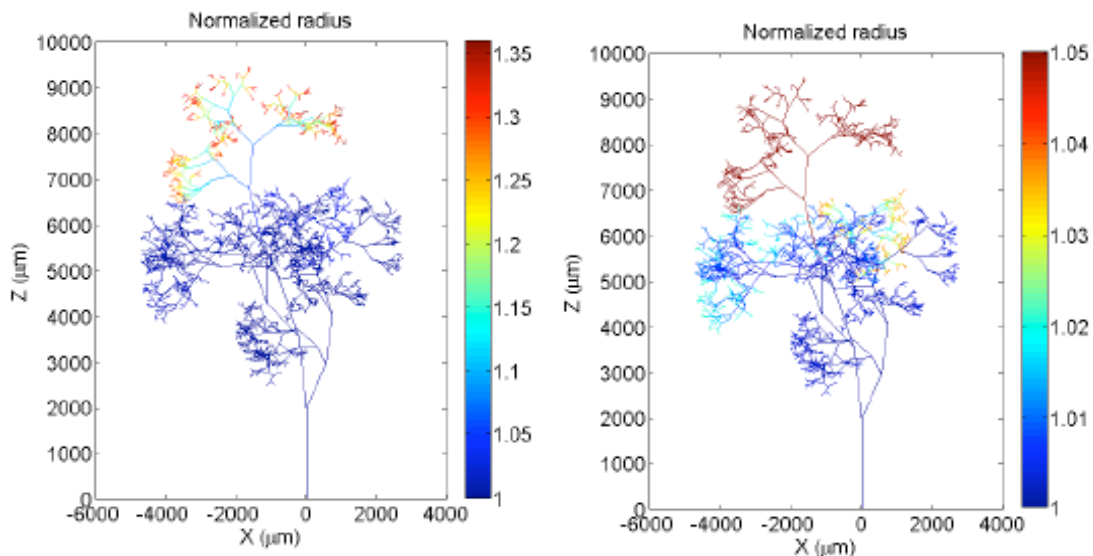


Figure 8 (left) relative change in radius, (right) relative change in radius with a compressed scale

Figure 8, left shows that the relative change in radius is largest in the smallest vessels of the tagged region. The maximal increase is approximately 35%. Hardly any response is visible in the non-tagged vessels. To investigate the response of the non-tagged vessels in more detail, Figure 8 right, shows the same situation with a smaller scale. It can be seen that the biggest changes take place in the vessels that are closest related to the tagged vessels i.e. the vessels that have the same antecedents as the tagged vessels. The largest relative change in the non-tagged vessels is approximately 4%.

To show the effect of varying the production rate locally we utilize a simple discontinuous function which switches, at $t = t_0$ the production rate that is proportional to a constant. At $t = t_1$, the value of the production rate is changed back to one i.e. to the initial condition. All values shown below are mean values (either averaged over all tagged and non-tagged vessels) and normalized to the initial condition.

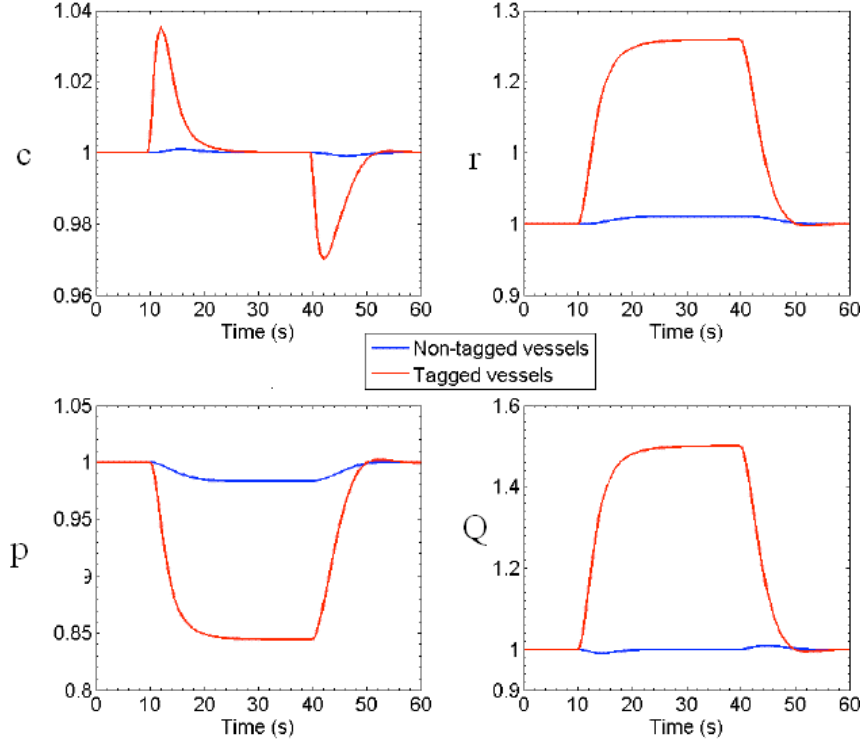


Figure 9 profiles for tagged and non-tagged vessels when local production rate is increased by 50%

Figure 9 shows the results for the tree when the local production rate is increased by 50%. The new steady state is reached at about $t = t_0 + 10$ with little or no oscillation (undershoot or overshoot) are visible. The same is true for the recovery after the production rate goes back to its initial value. In comparison with Figures 4a) and b) the full non-linear system shows virtually the same response to as the linearised analysis. This indicates that the asymmetry of the tree does not provide a large influence on the dynamics of the tree as a whole.

5 DISCUSSION AND CONCLUSIONS

We have presented a model of both geometry and dynamics of binary trees. The geometrical construction of 3D trees has been achieved through an amalgamation of work on staged growth by Karch [3] and the relationship of daughter/parenthood by Olufsen [2].

During the development of the concept of staged growth, different ways have been proposed to influence the direction in which the daughters of a segment grow and with it the geometry of the tree. The first choice that has been introduced is to use a powerlaw PDF or a normal PDF (see Figure 5). The powerlaw PDF has been chosen as an illustrative example but has a drawback in that it gives values for the components of the normal \mathbf{n} between 0 and λ . The normal PDF on the other hand results in a value (given by λ ,) but importantly with a variation. This results in a more 'natural' distribution of the component and gives more control over the direction of growth of the tree. Therefore, the normal PDF is the preferred PDF to use.

For the normal PDF, three different options have been proposed to scale the value between λ , and ε a random value chosen from a uniform distribution. These three different options have been analyzed in terms of branching angle (the angle that a daughter makes with its parent,). The distributions of the branching angles do not vary significantly between the different options.

The analysis of the z -coordinate of the terminal segments showed that option 2 gives the less satisfying results (negative z -coordinates results not shown). This can be explained by the hypothesis that the magnitude of the components of the normal \mathbf{n} is of more importance than the sign of this component for the direction of growth of the daughters. The results for options 1 and 3 show high similarity. However, it is advised to use option 1 in future research since this option gives components of the normal with both positive and negative values whereas option 3 gives only positive valued components.

Two different protocol functions have been analyzed in this study, the ramp function and the step function. The difference between the two functions is that the step function gives two clearly separated stages while the ramp function gives a continuous transition among many stages. This difference can be seen in the results shown in Figure 6. The tree generated with a step function as the protocol function grows during the first stage mainly in positive z -direction and spreads out in $(x-y)$ -direction during the second stage. This result indicates that a discontinuous protocol function can be used to create several, clearly separated stages of growth. Several opportunities have been shown to illustrate the working of the concept of staged growth. There are many more options available to acquire more control over the geometry of the tree, especially by choosing other (more complicated) protocol functions. The normal PDF shows the best results but a detailed analysis of the influence of the standard deviation in combination with different protocol functions is necessary. Figure 7 shows that by varying multiple components of the normal the direction of growth can be influenced in multiple directions but this has to be analyzed in more detail as well. Despite the fact that the concept of staged growth is a powerful tool to control the geometry of the tree, it has some drawbacks. The biggest drawback is that by choosing a normal \mathbf{n} , the daughters of a segment are forced to grow in a plane and not to grow in a certain direction. This gives the daughters still a relative large freedom to grow in an undesirable direction and is one of the reasons why the variation among trees generated with the same settings is large. Another reason is that it is a method based on random numbers and a small variation in these random numbers (especially for the largest, first created segments) has a large influence on the geometry of the entire tree.

Other simulations that have been performed simulated a local change of the “production” rate in the tree. The segments that changed their “production” rate are called tagged segments and two methods to tag segments have been developed. The results of the first method, region tagging, (results not shown) at the end of the simulation, the mean pressure and radius of the tagged segment differs from the initial value. This is unexpected and a possible explanation for this is the following. After the first change of the “production” rate (at $t = t_0$) the tree is not able to auto-regulate the “concentration”, c back to the initial value. The reason for this is probably that there are tagged segments that have non-tagged parent and daughter segments. The tagged segment reacts to the changed “production” by changing its radius but there is hardly any reaction in its parent and daughters because the segments are effectively uncoupled in this model. Because the limits to the radius are non-zero, the radius of the tagged segment can drift away from its setpoint value. This change is large enough such that the model cannot reach the initial steady state after the “production” rate goes back to its original value. Besides this, it has to be mentioned that the values for the tagged segments are averaged over less segments than the value for the non-tagged segments. It would be interesting to investigate the distribution of the radii at several moments during the simulations in combination with the averaged values. A more sophisticated way of tagging the segments would be a combination of both methods i.e. tag segments in a certain region and with them all their antecedents. In this way it will be possible to tag segments in a certain region and prevent the problems observed with the method of region tagging. However, it should be noted that it is difficult to find, a priori, a center for the region in which the segments get a tag. In this study, this has been solved by removing the random element in the code, visualizing the tree to select a region of interest and then run the code again. This is not possible with bigger trees since the computational cost to visualize them is too large for most computers.

All simulations in which the “production” rate is changed show that the relative change in flow is equal to the change in “production” rate. The response in the tree after a local “production” increase is visualized in Figure 8. The largest radius increase (relatively) occurs in the “production” activated region, which is expected from a physical point of view. However, this relative change is imposed by the ODE that describes the radius change (equation (1.36)) because the radius change is not a function of the radius itself. Therefore, when a large and a small segment experience the same concentration difference, their radius change will be the same in an absolute sense. When compared relatively however, the smallest segment will have a larger radius change and this can explain the results in Figure 8. As mentioned before, the “production” model used in this study is relatively simple. It can be extended in several ways. A first step can be the introduction of a myogenic model as done by Alzaidi [9] or the introduction of “concentrations” other than, thereby increasing the number of ODEs that have to be solved for each segment.

The concept of staged growth has been introduced in order to get more control of the geometry of the tree. Other options to get a more realistic geometry are the randomization of the radius and length-to-radius ratio of the segments, possibly in combination with the concept of staged growth. It is especially advised to make the tree more dense i.e. to create trees with more segments per unit volume. An experimental basis for this is the work performed by Lauwers *et al.* [10].

The proposed model can be coupled to other models, for example in order to create a model of the entire cerebral vasculature i.e. from the largest segments like the carotid arteries to the smallest segments, the capillary beds. Some of these models have been developed before, for instance the 3D, patient specific model of the Circle of Willis (CoW) developed by Moore *et al.* [11]. This model of the CoW can be combined with a model that simulates the pial arteries, possibly based on the vascular tree model developed in this study. The segments downstream of the pial arteries can be modeled as a vascular tree with the model developed in this study. Because a considerable amount of computational power is needed, it will be useful to develop the models such that they are compatible with a supercomputer. It is believed that this is the first model of a 3D tree that shows the response of a tree as a whole due to a local change in the “production” rate and it forms a basis for other models.

ACKNOWLEDGMENTS

We gratefully acknowledge the help of Nick Jaensson from the Centre for Bioengineering, University of Canterbury.

REFERENCES

1. Martini, F.H. “Fundamentals of anatomy and physiology”, Benjamin Cummings, 7th edition, 2005
2. Olufsen, M.S., M.S. Steele, and C.A. Taylor, Fractal Network model for simulating abdominal and lower extremity blood flow during reesting and exercise conditions. *Computer Methods in Biomechanics and Biomedical Engineering*, 2007. 10: p. 39-51.
3. R. Karch, F. Neumann, M. Neumann, and W. Schreiner. Staged growth of optimized arterial model trees. *Annals of biomedical engineering*, 28:495–511, 2000.
4. Schreiner, W. and P.F. Buxbaum, Computer-Optimization of Vascular Trees. *IEEE Trans Biomed Eng*, 1993. 40(5): p. 482-491.
5. Kamiya, A. and T. Togawa, Optimal Branching Structure of the Vascular Tree. *Bulletin of Mathematical Biophysics*, 1972. 34: p. 431-438.
6. Winitzki, S. “A handy approximation for the inverse error function and its inverse”. 2008. http://en.wikipedia.org/wiki/Error_function
7. Lapack++ Library for high performance linear algebra computations. <http://lapackpp.sourceforge.net/>.
8. David, T., H. Farr, and S. Alzaidi, Auto-regulation models of the cerebro-vasculature. *Journal of Engineering Mathematics*, 2009 DOI: 10.1007/s10665-009-9274-2
9. Alzaidi, S. “Autoregulation Models of the Circle of Willis”, PhD Thesis, University of Canterbury, New Zealand, 2009.
10. Lauwers, F., Cassot, F., Lauwers-Cances, V., Puwanarajah, P., and Duvernoy, H. *NeuroImage* 39, 936-948 (2008).
11. Moore, S. and T. David, *A model of autoregulated blood flow in the cerebral vasculature*. Proceedings of the IMechE part H, *Journal of Engineering in Medicine*, 2008. 222 (H4): p. 513-530.